

## COMMUNICATION

## Molecular Layer Deposition of Hybrid Siloxane Thin Films by Ring Opening of Cyclic Trisiloxane ( $V_3D_3$ ) and Azasilane

Received 00th January 20xx,  
Accepted 00th January 20xx

DOI: 10.1039/x0xx00000x

Kristina Ashurbekova,<sup>\*a</sup> Karina Ashurbekova,<sup>c</sup> Iva Saric,<sup>b</sup> Evgenii Modin,<sup>c</sup> Mladen Petradić,<sup>b</sup> Ilmutdin Abdulagatov,<sup>a</sup> Aziz Abdulagatov,<sup>a</sup> Mato Knez<sup>\*b,c,d</sup>

**In this work we report the first ring opening vapor to solid polymerization of cyclotrisiloxane and N-methyl-aza-2,2,4-trimethylsilacyclopentane by molecular layer deposition (MLD). This process was studied *in-situ* with a quartz crystal microbalance and the thin film was characterized by X-ray photoelectron spectroscopy, ATR-FTIR and High-resolution transmission electron microscopy.**

Silicon-based polymeric thin films have attracted a great interest because of their unique properties. Materials containing linear siloxane components and a linear siloxane skeleton show among the lowest elastic moduli reported.<sup>1</sup> Deposited by initiated chemical vapor deposition (i-CVD), siloxane films were shown to act as insulating layers in microelectronics,<sup>2, 3</sup> tunneling dielectric layers in thin film transistor-based organic flash memories,<sup>4</sup> thin film encapsulation layers,<sup>5</sup> biocompatible coatings,<sup>6–8</sup> thin film electrolytes for battery electrodes,<sup>9, 10</sup> or artificial solid electrolyte interface (SEI) layers.<sup>11</sup> All the mentioned application fields are expected to benefit from thin functional polymeric coatings with extreme precision in thickness on the nanometer scale.

Molecular layer deposition (MLD) is a thin film deposition technique that allows the growth of both pure organic and organic-inorganic hybrid thin films with a molecular level control over the film thickness and composition.<sup>12</sup> In contrast to other deposition techniques MLD is a non-line-of-sight deposition method, which enables conformal coatings of high aspect ratio micro- or nanostructures.<sup>13</sup> Highly chemically and thermally stable ultrathin carbosiloxane thin films with a low

dielectric constant were grown by MLD.<sup>14, 15</sup> The use of N-methyl-aza-2,2,4-trimethylsilacyclopentane as a precursor for surface functionalization and for atomic layer deposition (ALD) of  $SiO_2$  has been previously reported.<sup>16, 17</sup> First attempts to use cyclic siloxanes ( $D_3$ ,  $D_5$ ) to obtain polydimethylsiloxane (PDMS) by CVD were demonstrated by Abdulagatov *et al.*<sup>18</sup> A continuous growth of PDMS was expected through a constant ring opening polymerization reaction while dosing a cyclic siloxane. However, a growth termination and further mass loss after the precursor dosing was observed. In this work, molecular layer deposition has been used to deposit poly(Azasilane- $V_3D_3$ ) (poAV) thin films from 1,3,5-trivinyl-1,3,5-trimethylcyclotrisiloxane ( $V_3D_3$ ) and N-methyl-aza-2,2,4-trimethylsilacyclopentane.

A schematic of the proposed two-step MLD reaction of  $V_3D_3$  and azasilane is shown in Figure 1 (a). The experimental details are described in the supplementary information (SI). The MLD reaction (A) of azasilane with a hydroxylated surface is thermodynamically favored considering the bonding energies of Si–N and Si–O. The dissociation energy of a Si–N bond can range between 87 and 111 kcal mol<sup>−1</sup>, which is lower than that of a Si–O bond (122 to 136 kcal mol<sup>−1</sup>).<sup>17</sup> The reaction (B) of  $V_3D_3$  with the surface-terminating secondary amine from azasilane is opposite, involving Si–O bond dissociation and Si–N bond formation, as proposed in the magnified sketch in Figure 1 (a). The reactivity of the ring is triggered by the planar geometry of  $V_3D_3$ . According to DFT calculations, the  $D_3$  ring has 2.5 kcal mol<sup>−1</sup> of ring strain.<sup>19</sup> Therefore, the release of the ring strain energy might be one driving force for the ring opening polymerization (ROP) reaction. The ROP is also entropy-driven. The standard cyclization entropy  $\Delta S_c$  is negative, i.e. ring opening leads to an increase in entropy, due to a higher conformational freedom of the open polysiloxane chain.<sup>20</sup> Additional driving force might arise from the standard polymerization enthalpy  $\Delta H_p^0 = -3.6$  kcal mol<sup>−1</sup> and positive  $\Delta S_p^0 = 0.9$  cal mol<sup>−1</sup> K<sup>−1</sup> of  $D_3$  upon polymerization.<sup>21</sup> From the thermodynamic perspective, with  $\Delta G_p < 0$  a polymerization is possible.

<sup>a</sup>Dagestan State University, Makhachkala 36700, Russian Federation

<sup>b</sup>Department of Physics and Centre for Micro- and Nanosciences and Technologies, University of Rijeka, 51000 Rijeka, Croatia.

<sup>c</sup>CIC nanoGUNE, 20018 San Sebastian, Spain.

<sup>d</sup>IKERBASQUE, Basque Foundation for Science, 48013 Bilbao, Spain.

E-mail: [m.knez@nanogune.eu](mailto:m.knez@nanogune.eu), [krashurbekova@inbox.ru](mailto:krashurbekova@inbox.ru)

Electronic Supplementary Information (ESI) available: [MLD processing and characterization details]. See DOI: 10.1039/x0xx00000x

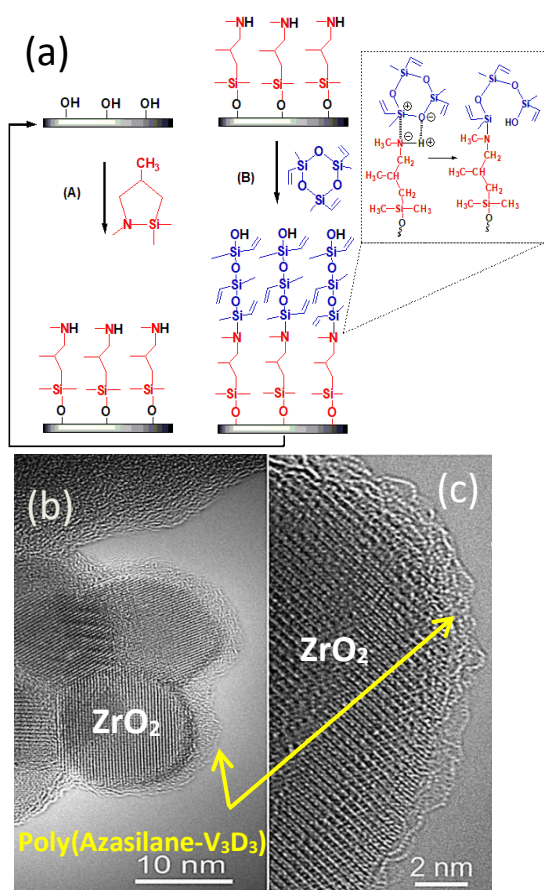


Figure 1 (a) Schematic of the proposed two-step MLD reaction of  $V_3D_3$  and azasilane; (b) TEM image of  $ZrO_2$  NPs after 150 MLD cycles of  $V_3D_3$  and azasilane at  $150\text{ }^\circ\text{C}$ ; (c) HR-TEM image of a  $ZrO_2$  NP surface after 150 MLD cycles of  $V_3D_3$  and azasilane at  $150\text{ }^\circ\text{C}$ .

Figure 1 (b), (c) shows transmission electron microscopy (TEM) images of poAV deposited on  $ZrO_2$  nanoparticles (NPs) by MLD.  $ZrO_2$  NPs were chosen for their chemical stability, high surface coverage with OH and good contrast in TEM images. The micrograph in Figure 1 (b) shows a nearly conformal coating of the  $ZrO_2$  NPs, characteristic of MLD processes.

The HRTEM image in Figure 1 (c) shows the chain-like nature of the deposit, manifesting a controlled growth of the polymeric (hybrid) material. Their shape confirms great molecular flexibility and stability, since the chains don't disaggregate upon irradiation with the focused electron beam. Figure 2 (a) shows the  $1800\text{--}750\text{ cm}^{-1}$  region of the ATR-FTIR spectrum of the as-deposited poAV thin film, grown at  $150\text{ }^\circ\text{C}$  with 150 MLD cycles (spectrum 2). Spectrum (1) shows pure  $ZrO_2$  NPs. The band between  $1250$  and  $1270\text{ cm}^{-1}$  is attributed to the symmetric bending of  $SiMe_x$  moieties, which is indicative of the bonding environment of silicon atoms. The peak shifts blue according to the degree of oxidation and level of substitution. Peaks centered at around  $1250$ ,  $1260$  and  $1270\text{ cm}^{-1}$  suggest mono-, di-, and tri-substituted groups, respectively.<sup>22</sup> The spectra of the poAV film show a strong and sharp peak at  $\sim 1258\text{ cm}^{-1}$ , suggesting di-oxygen substituted silicon atoms. Indeed, the silicon atom in  $V_3D_3$  contains a chain-building linear  $SiO_2MeVi$  unit. The signals related to vinyl

groups,  $=CH_2$  bending at  $1409\text{ cm}^{-1}$  and  $C=C$  stretching at  $1600\text{ cm}^{-1}$ , show the  $V_3D_3$  functional groups without changes during the process. The band at  $\sim 960\text{ cm}^{-1}$  is assigned to asymmetric Si-N stretching, confirming a reaction through Si-N bond formation between the surface-terminating secondary amine from azasilane and  $V_3D_3$ . Figure 2 (b) shows the  $C-H_x$  stretching region ( $3100\text{--}2700\text{ cm}^{-1}$ ) of the film. Also here, spectrum (1) and (2) show pure  $ZrO_2$  and as-deposited poAV, respectively. The bands within this region represent both symmetric and asymmetric methyl ( $-CH_3$ ) and methylene ( $-CH_2-$ ) stretching vibrations. Spectrum (2) in Figure 2 (a) shows an appearance of peaks at  $\sim 1067\text{ cm}^{-1}$ , an asymmetric stretching vibration of Si-O-Si. It is attributed to long-chain, network-type Si-O-Si moieties. The lack of the characteristic band of cyclotrisiloxanes at  $1012\text{ cm}^{-1}$  confirms an absence of such ring structures.<sup>23, 24</sup> Thermal ring opening of  $V_3D_3$  occurs at temperatures above  $500\text{ }^\circ\text{C}$ .<sup>6</sup> Thus, with a film growth at  $150\text{ }^\circ\text{C}$  a ROP via thermal decomposition can be excluded. This is further supported with the HRTEM image in Figure 1 (c), clearly showing a chain growth. Upon thermal decomposition

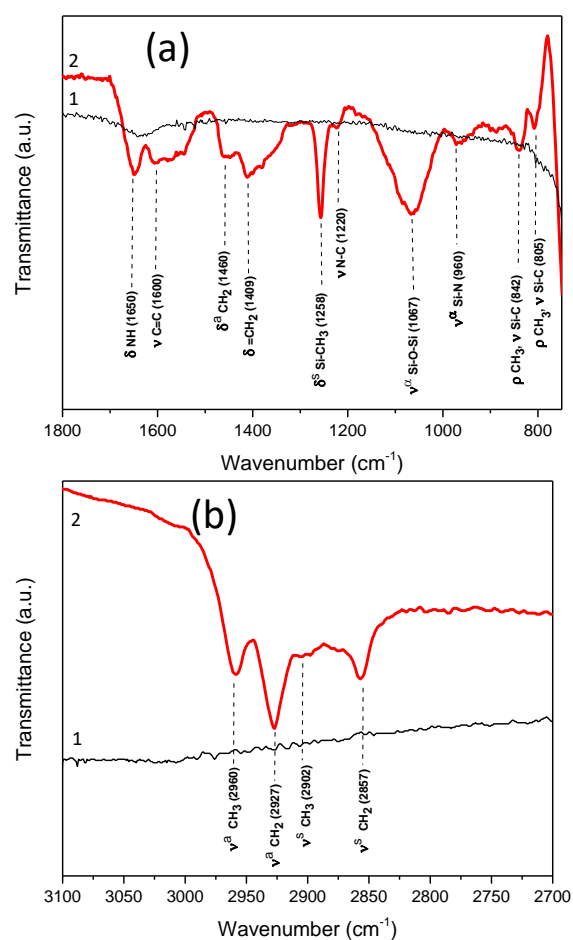


Figure 2 (a) Expanded view of the  $1800\text{--}750\text{ cm}^{-1}$  region of the ATR-FTIR spectra of: (1) pressed  $ZrO_2$  particle substrate prior to deposition and (2)  $ZrO_2$  after 150 cycles of  $V_3D_3$  and azasilane grown by MLD at  $150\text{ }^\circ\text{C}$ ; (b) expanded view of the  $2700\text{--}3100\text{ cm}^{-1}$  region of the ATR-FTIR spectra of (1) pressed  $ZrO_2$  particle substrate, prior to deposition, and (2)  $ZrO_2$  after 150 cycles of  $V_3D_3$  and azasilane MLD at  $150\text{ }^\circ\text{C}$ .

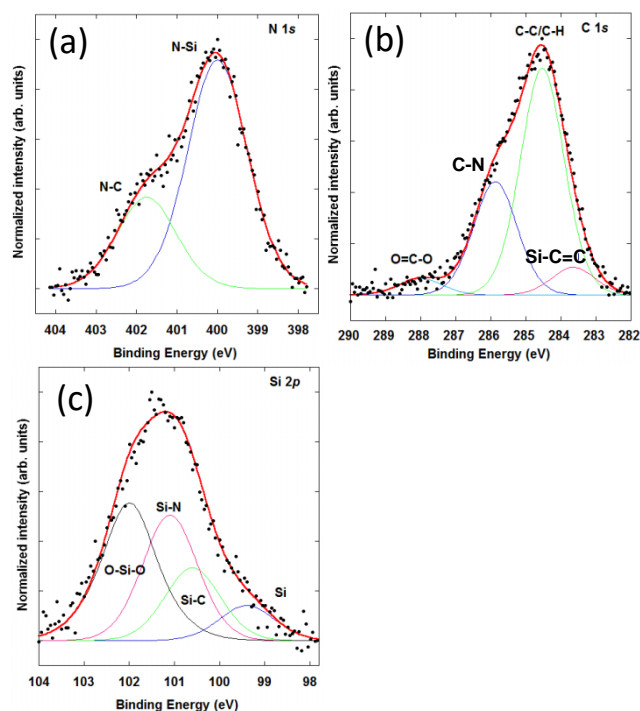


Figure 4 High-resolution XPS spectra of ZnO powder substrates coated with an MLD-deposited poly(Azasilane- $V_3D_3$ ) film around: (a) C 1s, (b) N 1s, and (c) Si 2p core-levels.

of the precursor rather individual aggregates would be seen. Both aspects confirm a ring opening mechanism.

The  $V_3D_3$  ring opening reaction was studied with *in-situ* QCM in a temperature range from 150 to 225 °C. The growth per cycle (GPC) of the poAV film vs. deposition temperature is shown in Figure S1 (SI). A maximum GPC of 14 ng  $cm^{-2}$  was observed at 200 °C. The GPC at 150 °C was lower and amounted to 8 ng  $cm^{-2}$ . No temperature “window” with a constant GPC was observed, which is typical for MLD processes.

Figure 3 (a) shows a mass gain versus time of  $V_3D_3$  and azasilane MLD in a steady state regime. A linear mass increase over MLD cycle numbers was observed. Figure 3 (b) shows an expanded view of the film growth at 150 °C that provides a constant growth per cycle of 8 ng  $cm^{-2}$ . Spikes in the graph (< 1 ng  $cm^{-2}$ ) originate from noise. The nucleation of the film growth was studied with *in-situ* QCM on a 7 nm thick  $Al_2O_3$  film grown onto the quartz crystal surface by ALD. The QCM measurements of the mass gain (MG) vs. time for the poAV growth during the first 10 reaction cycles at 150 °C is shown in Figure S2 (SI). The GPC reduces from 22 ng/ $cm^2$  to a constant value of 8 ng/ $cm^2$  within 9 reaction cycles, demonstrating a linear growth in a steady regime. Such nucleation behavior, where the GPC is higher in the initial stage of the growth than in the steady regime confirms an MLD-typical substrate-enhanced growth type, which occurs when the number of reactive sites on the substrate is higher than on the MLD-grown material. The film nucleation was studied on ALD-grown  $Al_2O_3$ , which has among the highest concentration of surficial hydroxyl groups within ALD-grown materials. The total range

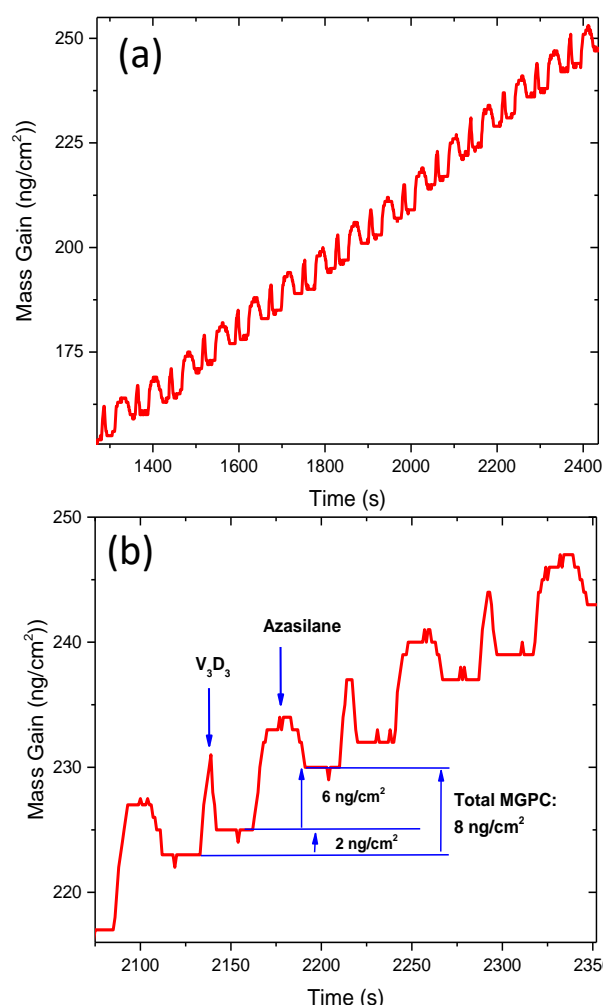


Figure 3 (a) QCM measurements of mass gain versus time for an MLD reaction of  $V_3D_3$  and azasilane: growth over 15 reaction cycles in a steady state regime at 150 °C; (b) expanded view of a growth at 150 °C during three reaction cycles.

of the QCM measurements of mass gain vs. time for the poAV growth during 45 cycles at 150 °C is shown in Figure S3 (SI).

The self-limiting behavior of the surface reactions was studied at 150 °C. The QCM results showing the mass gain per cycle vs. Azasilane and  $V_3D_3$  dosing time are shown in Figure S4 (a) and S4 (b) (SI), respectively. The precursor dosing times were within the saturation regime, since no change in the growth dynamics was observed with values larger than 5s and 3s for Azasilane and  $V_3D_3$ , respectively. X-ray Reflectivity (XRR) showed a root mean square roughness of 0.6 nm for a 9 nm thick poAV film grown on a Si wafer. At 150 °C the process exhibited a GPC of  $\sim 0.6$  Å/cycle and the resulting film had a density of 2.6 g  $cm^{-3}$  as deduced from XRR measurements.

The overall composition and bonding environment in the deposited MLD film was assessed by x-ray photoelectron spectroscopy (XPS) of a pressed ZnO powder substrate, coated with 90 Å (150 MLD cycles) of  $V_3D_3$  and azasilane. ZnO was used instead of  $ZrO_2$ , because it shows intrinsic conductivity, which minimizes charging effects for more accurate XPS measurements. The XPS spectra, measured around C 1s, N 1s

or Si 2p core-levels, were deconvoluted into sets of mixed Gaussian-Lorentzian (G-L) functions with Shirley background subtraction.<sup>25</sup> The assignment for each of the fitting peaks is shown in Figure 4. The C 1s spectrum in Figure 4 (a) shows several components originating from differently bound carbon within the MLD film. These components were assigned to Si-C=C, C-C, C-N or O-C=O (surface contamination) bonds at binding energies (BEs) of 283.6 eV, 284.5 eV, 285.9 eV or 288.0 eV, respectively. The XPS around N 1s core-levels in Figure 4 (b) was deconvoluted into two components from two different N-containing bonding combinations. The contributions at BEs of 401.7 and 400.0 eV are characteristic of N-C and N-Si bonds, respectively. The very presence of a N-Si peak around N 1s core-levels confirms the reaction between V<sub>3</sub>D<sub>3</sub> and azasilane in the deposited MLD film. Finally, the spectrum around Si 2p core-levels in Figure 4 (c) shows several Si bonding environments. The curve was deconvoluted into four components, assigned to four silicon-related bonding situations: Si-O, Si-N, Si-C or Si, at BEs of 102.0 eV, 101.1 eV, 100.6 eV, and 99.4 eV, respectively. The dominant peak in the Si 2p photoemission at 102.0 eV is assigned to the Di-oxygen substituted state of Si.<sup>26</sup> Thus, the XPS analysis reveals all chemical components expected in the poAV MLD film.

In this study, a ring opening copolymerization of cyclotrisiloxane (V<sub>3</sub>D<sub>3</sub>) and cyclic azasilane by MLD was developed. *In-situ* QCM showed a linear MLD film growth regime and self-limiting behaviour for both MLD surface reactions. ATR-FTIR and XPS analyses both confirmed the presence of Si-N bonds, indicating a surface reaction through V<sub>3</sub>D<sub>3</sub> ring opening and Si-N bond formation with the secondary amine of azasilane. The ring strain and entropy in V<sub>3</sub>D<sub>3</sub> appear to play an enabling role, which gives an important input for future considerations of ROP reactions performed by MLD, since strained rings can lower the processing temperature due to higher reactivity of the molecule. HR-TEM imaging confirmed the conformal nature of the deposited MLD film and a controlled chain growth.

This investigation contributes significantly to the pool of applicable MLD reactions, widening the usable chemistries and offering additional materials to grow. Especially for flexible electronics and further applications where functional nanoscale polymeric coatings will be of importance, our approach allows more flexibility in the design of the processes and the resulting polymer films. The obtained thin films have potential applications as low-k materials, biocompatible, and flexible electrode coating material. The vinyl groups from V<sub>3</sub>D<sub>3</sub> allow further functionalization, for example attachment of further functionalities or even cross-linking, which will be investigated in forthcoming work.

#### Conflicts of interest

There are no conflicts to declare

#### Acknowledgements

M.K. acknowledges funding from the Spanish Ministry of Economy and Competitiveness (MINECO) [MAT2016-77393-R], incl. FEDER funds, and the Maria de Maeztu Units of Excellence Programme

[MDM-2016-0618]. Ka.A. acknowledges funding through European Union's H2020 R&I programme under the Marie Skłodowska-Curie [765378]. I.S., M.P. and M.K. acknowledge the University of Rijeka support under the project number 18-144.

#### Notes and references

1. N. Takano, T. Fukuda and K. Ono, *Polym. J.*, 2001, **33**, 469.
2. H. Moon, H. Seong, W. C. Shin, W.-T. Park, M. Kim, S. Lee, J. H. Bong, Y.-Y. Noh, B. J. Cho, S. Yoo and S. G. Im, *Nat. Mater.*, 2015, **14**, 628.
3. K. Pak, H. Seong, J. Choi, W. Hwang and S. Im, *Adv. Funct. Mater.*, 2016, **26**, 6574.
4. S. Lee, H. Seong, S. G. Im, H. Moon and S. Yoo, *Nat. Commun.*, 2017, **8**, 725.
5. B. Jun Kim, H. Seong, H. Shim, Y. Il Lee and S. Im, *Adv. Eng. Mater.*, 2017, **19**, 1600870
6. W. S. O'Shaughnessy, M. Gao and K. K. Gleason, *Langmuir*, 2006, **22**, 7021.
7. W. S. O'Shaughnessy, S. K. Murthy, D. J. Edell and K. K. Gleason, *Biomacromolecules*, 2007, **8**, 2564.
8. A. Achyuta, V. S. Polikov, A. White, H. Pryce Lewis and S. K. Murthy, *Macromol. Biosci.*, 2010, **10**, 872.
9. N. Chen, B. Reeja-Jayan, J. Lau, P. Moni, A. Liu, B. Dunn and K. K. Gleason, *Mater. Horiz.*, 2015, **2**, 309.
10. N. Chen, B. Reeja-Jayan, A. Liu, J. Lau, B. Dunn and K. K. Gleason, *Macromol. Rapid Comm*, 2016, **37**, 446.
11. B. H. Shen, S. Wang and W. E. Tenhaeff, *Sci. Adv.*, 2019, **5**, eaaw4856.
12. K. Gregorczyk and M. Knez, *Prog. in Mat. Sci.*, 2016, **75**, 1.
13. S. M. George, B. Yoon and A. A. Dameron, *Acc. Chem. Res.*, 2009, **42**, 498.
14. H. Zhou and S. F. Bent, *J. Phys. Chem. C*, 2013, **117**, 19967.
15. R. G. Closser, D. S. Bergsman and S. F. Bent, *ACS Appl. Mater. Inter.*, 2018, **10**, 24266.
16. L. Ju and N. C. Strandwitz, *J. Mater. Chem. C*, 2016, **4**, 4034.
17. A. Maddox, J. Matison, M. Singh, J. Zazyczny and B. Arkles, *MRS Proceedings*, 2015, **1793**, 35.
18. A. I. Abdulgatov, *Chemistry & Biochemistry Graduate Theses & Dissertations. 83.*, 2012.
19. T. B. Casserly and K. K. Gleason, *J. Phys. Chem. B*, 2005, **109**, 13605.
20. R. G. Jones, W. Ando and J. Chojnowski, *Springer Science+Business Media Dordrecht*, 2000, 763.
21. B. M. Mandal, *Fundamentals of Polymerization*, World Scientific, 2013.
22. D. D. Burkey and K. K. Gleason, *J. Appl. Phys.*, 2003, **93**, 5143.
23. A. K. H. Achyuta, A. J. White, H. G. Pryce Lewis and S. K. Murthy, *Macromolecules*, 2009, **42**, 1970.
24. G. Aresta, J. Palmans, M. C. M. v. d. Sanden and M. Creatore, *J. Vac. Sci. Technol. A*, 2012, **30**, 041503.
25. R. Hesse, T. Chassé and R. Szargan, *Fresen. J. Anal. Chem.*, 1999, **365**, 48.
26. L.-A. O'Hare, A. Hynes and M. R. Alexander, *Surf.Interface Analysis*, 2007, **39**, 926.